Generalized single excitation configuration interaction: an investigation into the impact of the inclusion of non-orthogonality on the calculation of core-excited states

Journal:	*Physical Chemistry Chemical Physics*
Manuscript ID	CP-ART-12-2019-006592.R1
Article Type:	Paper
Date Submitted by the Author:	06-Mar-2020
Complete List of Authors:	Oosterbaan, Katherine; University of California Berkeley, White, Alec; California Institute of Technology Hait, Diptarka; University of California, Berkeley, Chemistry Head-Gordon, Martin; UC Berkeley

Generalized single excitation configuration interaction: an investigation into the impact of the inclusion of non-orthogonality on the calculation of core-excited states

Katherine J. Oosterbaan, Diptarka Hait, and Martin Head-Gordon
Department of Chemistry, University of California,
Berkeley, California 94720, USA and
Chemical Sciences Division, Lawrence Berkeley
National Laboratory, Berkeley, California 94720, USA

Alec F. White
Division of Chemistry and Chemical Engineering,
California Institute of Technology, Pasadena, California 91125, USA

Abstract

In this paper, we investigate different non-orthogonal generalizations of the configuration interaction with single substitutions (CIS) method for the calculation of core-excited states. Fully non-orthogonal CIS (NOCIS) has been described previously for species with singlet and doublet ground states, and this paper reports the extension to molecules in their triplet ground state. In addition to NOCIS, we present a novel method, one-center NOCIS (1C-NOCIS), for open-shell molecules which is intermediate between NOCIS and the computationally less demanding static exchange approximation (STEX). We explore this hierarchy of spin-pure methods for core excitations of molecules with singlet, doublet, and triplet ground states. We conclude that, while NOCIS provides the best results and preserves the spatial symmetry of the wavefunction, 1C-NOCIS retains much of the accuracy of NOCIS at a dramatically reduced cost. For molecules with closed-shell ground states, STEX and 1C-NOCIS are identical.

I. INTRODUCTION

X-ray absorption spectroscopy (XAS) is a highly useful and widely used method, due in large part to its element specificity and sensitivity to chemical environment[1,2]. Sensitivity to environment also makes XAS a powerful reporter on excited states and electron dynamics[3,4]. In addition to synchrotron-based experiments, smaller laboratory-scale XAS set-ups are also now being used in time-resolved experiments[5]. In light of this, the identification of characteristic XAS peaks of molecular species is of growing significance for experimentalists and theorists alike. This is especially true for species with an open-shell ground state, which have so far been less studied, and chemists face the difficult job of both assigning peaks and also identifying the source of peak shifts[6]. Theoretical calculations with a good balance of efficiency and accuracy can greatly facilitate the task of assigning XAS spectra.

There are many different approaches to calculations of core-excited states[7]. Early methods used multiple scattering X_α[8] and transition potential calculations[9], but since then ab-initio quantum methods have dominated the field. Currently, the common methods used for core excitations are time-dependent density functional theory (TDDFT)[10–15], Δ-SCF and Δ-DFT[16], coupled-cluster methods[17–28], algebraic diagrammatic construction (ADC) methods[29–35], and configuration interaction singles (CIS)[36–38]. The general benefits and pitfalls of all these methods have been discussed elsewhere[11,20,34], but we would like to focus on multi-state, spin-pure, wavefunction-based methods that are cheaper than ADC and CC methods. To do so, we first look at the static exchange (STEX) method[39–41], which has been around for some time. The specific theory will be discussed more later, but of particular relevance is that in molecules with multiple equivalent atoms (eg. the two O 1s K-edges in CO_2) STEX considers the coupling between non-orthogonal determinants to be negligible. This makes STEX an exceptionally efficient method from a computational standpoint.

A natural extension of STEX is to include the coupling between non-orthogonal configurations, which we have termed non-orthogonal configuration interaction singles (NOCIS)[42–44]. The theory is discussed in Section II. The inclusion of this coupling can be especially important for computing XAS spectra of doublet molecules[44] and in this work we reiterate this point and show that it is similarly important for triplet molecules. At the same time, the increased complexity of the method means that it is more computationally demanding than STEX.

The purpose of this paper is to explore the impact of the coupling between non-orthogonal determinants on the calculation of core-excited states. To do so, we investigate the difference between the fully non-orthogonal method (NOCIS), a method that includes partial non-orthogonality (one-center, or 1C-NOCIS), and a fully orthogonal method (STEX) on molecules with singlet, doublet, and triplet ground states. The theory and implementation of 1C-NOCIS and of NOCIS for molecules with a triplet ground state has not been previously reported. We found that while NOCIS is the most accurate and has the advantage of not breaking spatial symmetry, the 1C-NOCIS method provides the best cost to benefit ratio for computing core-excited states, retaining some important aspects of non-orthogonality at a greatly reduced cost. We also demonstrate the practicality of 1C-NOCIS by computing XAS spectra of some medium-sized open-shell molecules.

II. THEORY

A. NOCIS

The motivation for NOCIS is the desire to improve on CIS while still maintaining a reasonably low computational scaling. It does so by including orbital relaxation, which CIS neglects altogether, and the non-orthogonal interaction between multiple core-hole references, such as the O $1s$ orbitals in O_2.

A brief overview of the NOCIS algorithm is as follows: after a ground-state orbital optimization, a Maximum Overlap Method (MOM)[45] or a Square Gradient Minimization (SGM)[46] calculation is done for an ionization from each localized core orbital of interest. This introduces orbital relaxation, and also renders the excited states non-orthogonal to the ground state. The Hamiltonian, overlap, and total spin squared matrices are constructed using the Slater-Condon rules for matrix elements between determinants which share a common set of orbitals and NOCI for the remaining matrix elements[47]. Finally, the generalized eigenvalue problem is solved.

NOCIS is spin-pure, size consistent, and maintains spatial symmetry. Like CIS, NOCIS produces excited states with the same m_s as the reference but potentially with larger total spin. For example, performing NOCIS on a molecule with a singlet ground state will produce both singlet and triplet excited states. In previous papers[42,44], we implemented NOCIS for

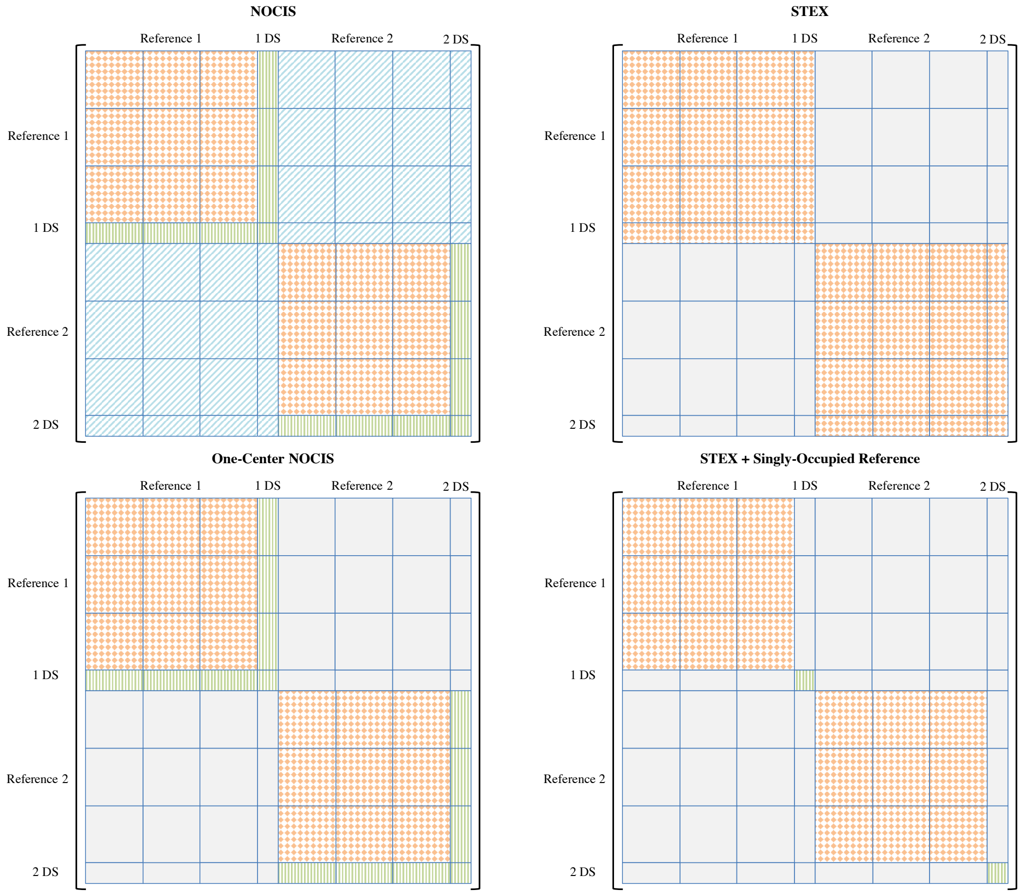

FIG. 1. A visual representation of the Hamiltonian matrices for each method for a two-reference doublet molecule (i.e. containing two atoms of a target element). The peach/diamond components are computed with orthogonal Slater-Condon rules, the blue/diagonal stripe elements are obtained with NOCI from the ionized determinants, and the green/vertical stripe elements are obtained with NOCI from the determinants that are excited into the open-shell orbital. The gray elements are zero.

molecules with singlet and doublet ground states. We provide a brief summary of these methods here.

NOCIS for core excitations from a singlet ground state has the following wavefunction:

$$|\Psi_{NOCIS}\rangle = \sum_{i=1}^{R}\sum_{a=1}^{V} \mathbf{t}_i^a (1-\hat{\mathbf{P}})[\hat{a}_a^\dagger \hat{a}_i \pm \hat{a}_{\bar{a}}^\dagger \hat{a}_{\bar{i}}]|\Phi_i\rangle \tag{1}$$

In singlet NOCIS, the wavefunction is constructed starting from R different core-ionized determinants corresponding to core electron removal from each identical atom of interest and ROHF optimization of those cation determinants, our $|\Phi_i\rangle$. Alpha and beta electrons are then added into each of the V virtual orbitals (different for each cation determinant), and the resulting core-excited configuration is projected against the closed-shell ground state determinant to ensure that the core-excited states are strongly orthogonal to the ground state. In Equation 1, $\mathbf{t}_i^a$ are the amplitudes defining the NOCIS wavefunction of a particular core excited state that we are solving for, $\hat{\mathbf{P}}$ is the ground-state projector, and $\hat{a}_a^\dagger$ and $\hat{a}_i$ are the standard creation and destruction operators. A bar over the subscript indicates a beta electron.

In NOCIS for core excitations from doublet ground states, we begin to have to contend with ground-state open-shell orbitals in order to fully consider all possible single excitations. This involves the addition of another reference, which we term DS, indicating an excitation from a doubly occupied (D) core orbital to a singly-occupied (S) valence orbital.

$$|\Psi_{NOCIS}\rangle = \sum_{i=1}^{R}\sum_{a=1}^{V}(1-\hat{\mathbf{P}})\left(\mathbf{t}_i^a[a_a^\dagger a_i] + \mathbf{t}_{\bar{i}}^{\bar{a}}[a_{\bar{a}}^\dagger a_{\bar{i}}] + \mathbf{t}_{\bar{i}k}^{\bar{k}a}[a_{\bar{k}}^\dagger a_{\bar{i}} a_a^\dagger a_k]\right)|\Phi_i\rangle + \sum_{i=1}^{R}\mathbf{t}_i^k(1-\hat{\mathbf{P}})[a_{\bar{k}}^\dagger a_{\bar{i}}]|\Phi_i^k\rangle \tag{2}$$

There are a few changes of note when contrasting doublet and singlet NOCIS. The first is within the space of the original reference, $|\Phi_i\rangle$. In order to maintain spin-purity, we now feature an excitation that can be considered a double excitation, which is an XCIS-type extension[48], and moves us beyond the space of purely single excitations. Additionally, we can see the DS reference separately optimized, with k being the ground-state open-shell orbital. Because of this, the second and first terms are mutually non-orthogonal, which introduces additional non-orthgonality to our matrices. The notation in this equation is identical to that for Eq. 1 for the singlet ground state case.

In this work we have also implemented the extension of NOCIS to molecules with triplet ground states. As with doublet NOCIS, triplet NOCIS once again expands the number of configurations necessary to maintain spin-purity for the $m_s = +1$ state. This includes an additional reference for the second singly-occupied ground-state orbital. These excitations are visualized in Figure 2. The triplet NOCIS wavefunction is as follows:

$$\begin{aligned}|\Psi_{NOCIS}\rangle = \sum_{i=1}^{R}\sum_{a=1}^{V}(1-\hat{\mathbf{P}})\left(\mathbf{t}_i^a[a_a^\dagger a_i] + \mathbf{t}_{\bar{i}}^{\bar{a}}[a_{\bar{a}}^\dagger a_{\bar{i}}] + \mathbf{t}_{\bar{i}j}^{\bar{j}a}[a_{\bar{j}}^\dagger a_{\bar{i}} a_a^\dagger a_j] + \mathbf{t}_{\bar{i}k}^{\bar{k}a}[a_{\bar{k}}^\dagger a_{\bar{i}} a_a^\dagger a_k]\right)|\Phi_i\rangle \\ + \sum_{i=1}^{R}\mathbf{t}_i^j(1-\hat{\mathbf{P}})[a_{\bar{j}}^\dagger a_{\bar{i}}]|\Phi_i^j\rangle + \sum_{i=1}^{R}\mathbf{t}_i^k(1-\hat{\mathbf{P}})[a_{\bar{k}}^\dagger a_{\bar{i}}]|\Phi_i^k\rangle\end{aligned} \tag{3}$$

The notation in this equation is identical to Eq. 1 for singlet ground states.

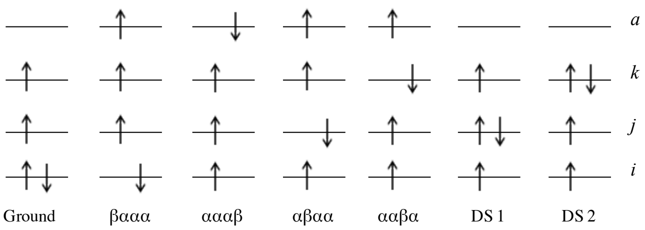

FIG. 2. All potential triplet core-excitations for spin-completeness. i is a core orbital, j and k are the singly-occupied ground-state orbitals, and a is a virtual orbital. Three different sets of optimized orbitals are employed: core ionized orbitals for the core-to-virtual excitations and a specifically optimized set for each core-to-singly occupied configuration (DS 1 and DS 2 above).

B. Static Exchange

In the simplest form of STEX[39], one computes excitation energies by diagonalizing the virtual space of a Fock matrix for the ionized system. This method is especially attractive for computing x-ray spectra[40,49] for many of the same reasons as NOCIS: it achieves much-improved results over conventional CIS, while being very computationally cheap, particularly relative to correlated methods such as ADC or EOM-CC. At present, however, STEX is not systematically improvable[7] in the same way as NOCIS, which has more avenues for the addition of dynamic correlation such as NOCI-MP2[50].

When using STEX on multiple core-ionized states as done, for example, by Ågren et al.[49], the underlying assumptions are that the coupling between non-orthogonal determinants is negligible, and that all relevant excited determinants can be formed by single electron-attachment to the core-ionized state. In this way, STEX can be considered to be an approximation to NOCIS.

In our implementation of STEX, we follow an algorithm very similar to NOCIS. Our ground-state calculation includes the Boys localization of the reference orbitals before the MOM/SGM calculation. However, as can be seen in Figure 1, we form the DS reference from the core-ionized reference, instead of optimizing it separately. This renders the DS state orthogonal to the rest of the core-excitations from that particular atom. After the matrix build, we project the orthogonal matrix blocks against the ground state (contrasted with NOCIS, where the whole matrix is projected against the ground state), and solve the eigenvalue problem. Because the basis of excited determinants is not orthogonal to the ground state, NOCI is required to compute the oscillator strengths[41]. We also explored a method (referred to as STEX + Single Reference in Figure 1) where we separately optimized the DS reference as in NOCIS, but ignored the coupling between the resulting non-orthogonal determinants.

Like NOCIS, STEX is spin-pure and size-consistent. However, due to the de-coupling of the references, STEX calculations break the spatial symmetry of the final states, which can slightly skew the results (see Section III). It is also important to note that STEX has been known to compress spectra due to a lack of polarization effects, believed to be due to neglecting the screening effects of the excited electron, which causes the lowest core-excited states to be over-screened[7,51]. NOCIS and 1C-NOCIS do not contain any explicit fix to this problem, and so may also exhibit this behavior (although the results presented later do not appear to be affected in this way).

C. One-Center NOCIS

To explore the effect of different types of non-orthogonality, we introduce another approximate method, one-center NOCIS (1C-NOCIS), which is an intermediate between NOCIS and STEX. The "DS" determinants are separately optimized as in NOCIS, but the coupling between non-orthogonal determinants with core holes on different centers is ignored. This is depicted in Figure 1, and NOCI is used to compute the remaining matrix elements between non-orthogonal determinants. 1C-NOCIS constructs the orthogonal Slater-Condon components of the matrices, and then performs NOCI to obtain the relevant non-orthogonal components. The diagonal blocks are then projected against the ground state.

For singlet NOCIS, 1C-NOCIS is the same as STEX, since there are no open-shell ground-state orbitals. As can be seen in Figure 1, for a doublet ground state this results in a column of matrix elements that must be computed using NOCI. For triplet molecules there are two such columns corresponding to the two open-shell orbitals of the ground state. It is easy to imagine how this could be generalized as the number of ground-state open-shell orbitals increases.

There are two main advantages of 1C-NOCIS. First, it is substantially cheaper to evaluate than NOCIS and so enables the treatment of larger molecules. Crucially, in most systems we examine below, the coupling between excited determinants that is neglected in 1C-NOCIS is verified to be very small, so the accuracy of NOCIS is retained. Second, and in contrast to STEX, it allows the DS states to relax separately, which we have already shown to be important in NOCIS for core excitations on molecules with doublet ground states[44]. We will present additional examples below.

D. Computational Implementation

The code for NOCIS, 1C-NOCIS, and STEX is implemented in a development version of Q-Chem 5.0[52] utilizing the Armadillo linear algebra library[53]. The NOCI code is a further modified version of the code developed by Sundstrom[54] and adapted by Oosterbaan et al.[42]. NOCIS scales as $\frac{1}{2}A(A-1)V^2N^2$, where A is the number of atoms of interest, V is the number of virtual orbitals, and N is the number of basis functions. 1C-NOCIS and STEX scale as AVN^2, which is a substantial improvement.

III. RESULTS

All geometries are obtained from NIST's Computational Chemistry Comparison and Benchmark Database[55], which are optimized using B3LYP[56–58] in the Def2-TZVPD basis set[59], except those in the Larger Cases section, which are optimized in Q-Chem using the same basis set and functional. Single-reference molecules are defined as molecules with only one equivalent atom (eg. the O K-edge in CO). Multi-reference molecules have more than one of the same atom of interest (eg. the O K-edge in CO_2), and thus result in larger matrix dimensions and a further introduction of non-orthogonality. We defined the K-edge as the lowest state with nonzero oscillator strength.

A. Benchmarks

For singlet molecules with single core-hole references, NOCIS, 1C-NOCIS, and STEX methods are identical. Additionally, 1C-NOCIS and STEX are identical for all singlet ground-state molecules. Thus, for singlet molecules we compare NOCIS and 1C-NOCIS/STEX for multiple core-hole reference molecules. The results can be seen in Tables

Molecule	Experiment	NOCIS	STEX/1C-NOCIS (dif. from NOCIS)
N_2 N(1s)	400.96[60]	404.529	0.013
F_2 F(1s)	682.2[61]	685.485	0.015
C_2H_2 C(1s)	285.9[62]	289.747	0.023
C_2H_4 C(1s)	284.68[62]	288.677	0.005
C_2H_6 C(1s)	286.9[62]	292.135	0.006
CO_2 O(1s)	535.3[63]	538.045	0.000
C_3H_8 C(1s)	-	292.135	0.001
C_3H_6 C(1s)	-	288.984	0.000
C_3H_4[a] C(1s)	-	289.597	0.000
C_3H_4[b] C(1s)	-	290.097	0.003
MSE from NOCIS		-	0.007
RMSE from NOCIS		-	0.010
RMSE from Expt.		3.857	3.867

[a] allene

[b] propyne

TABLE I. A comparison of NOCIS singlet K-edge energies and 1C-NOCIS/STEX K-edge differences in the 6-31G[64,65] basis set, and a further comparison to available experimental data. Mean signed error (MSE) and root mean square error (RMSE) are included. For singlet molecules, 1C-NOCIS and STEX are identical.

1 and 2.

The outcome of this is quite clear: while the NOCIS results are always lower in energy, the 1C-NOCIS/STEX results are very close to or the same as the NOCIS numbers, and in all cases are the same up to one decimal place, which is enough to identify a potential XAS K-edge. Thus, we conclude that multiple core-hole reference singlet molecules have a low degree of configuration interaction between configurations corresponding to core excitations from different atoms, and 1C-NOCIS/STEX is a more efficient way to obtain reasonably accurate results.

For doublet molecules with single core-hole references, 1C-NOCIS and NOCIS are iden-

Molecule	Experiment	NOCIS	STEX/1C-NOCIS (dif. from NOCIS)
N_2 N(1s)	400.96	402.119	0.019
F_2 F(1s)	682.2	683.601	0.014
C_2H_2 C(1s)	285.9	287.164	0.028
C_2H_4 C(1s)	284.68	286.380	0.007
C_2H_6 C(1s)	286.9	287.423	0.007
CO_2 O(1s)	535.3	536.096	0.000
C_3H_8 C(1s)	-	287.420	0.001
C_3H_6 C(1s)	-	286.749	0.001
C_3H_4[a] C(1s)	-	287.330	0.003
C_3H_4[b] C(1s)	-	287.517	0.003
MSE from NOCIS		-	0.008
RMSE from NOCIS		-	0.012
RMSE from Expt.		1.204	1.217

[a] allene

[b] propyne

TABLE II. A comparison of NOCIS singlet K-edge energies and 1C-NOCIS/STEX K-edge differences in the aug-cc-pCVTZ[66–68] basis setand a further comparison to available experimental data. Mean signed error (MSE) and root mean square error (RMSE) are included. For singlet molecules, 1C-NOCIS and STEX are identical.

tical. For multiple core-hole reference cases, the 1C-NOCIS matrices take the form of diagonal blocks as seen in Figure 1. This dramatic reduction of NOCI calculations provides a substantial speedup in computation time. The comparison results in the 6-31G[64,65] and aug-cc-pCVTZ basis sets can be seen in Tables 3 and 4, respectively. There does not appear to be an appreciable change in the 1C-NOCIS/NOCIS differences on increasing the basis set size.

There are a few items of note in these results. The first is that the NOCIS-STEX differences are markedly larger for doublet molecules than for singlet ones. This is due to the fact that the DS reference state is not optimized alone, and is instead formed from the core-

Molecule	Experiment	NOCIS	STEX (dif. from NOCIS)	1C-NOCIS (dif. from NOCIS)
HO_2 O(1s)	528.6[6]	531.710	1.179	0.000
N_2^+ N(1s)	-	397.679	0.341	-0.031
C_2H_3 C(1s)	-	285.601	0.493	0.000
NO N(1s)	399.7[69]	403.316	0.946	0
NO O(1s)	532.7[69]	534.956	0.000	0
NO_2 N(1s)	401.04[70]	404.610	0.842	0
NO_2 O(1s)	530.32[70]	532.775	0.966	0.001
OH O(1s)	525.8[6]	529.833	1.654	0
CH_3 C(1s)	281.35[71]	284.967	1.036	0
CN C(1s)	-	283.797	0.076	0
CN N(1s)	-	396.910	0.706	0
HCO C(1s)	-	288.470	0.697	0
HCO O(1s)	-	534.023	0.504	0
N_2O^+ O(1s)	-	531.955	1.148	0
CO_2^+ C(1s)	-	292.651	0.000	0
CO_2^+ O(1s)	-	530.433	0.955	-0.001
MSE from NOCIS		-	0.721	-0.002
RMSE from NOCIS		-	0.850	0.007
RMSE from Expt.		3.294	4.301	3.294

TABLE III. A comparison of NOCIS doublet K-edge energies and STEX K-edge and 1C-NOCIS differences in the 6-31G[64,65] basis set, and a further comparison to available experimental data. Mean signed error (MSE) and root mean square error (RMSE) are included. A 0 in the 1C-NOCIS column indicates that 1C-NOCIS and NOCIS are identical in that case.

ionized reference. In previous work[44], we found that doing this substantially decreased the accuracy of our results, and that far more accurate results could be obtained by separately optimizing the DS reference. A more accurate DS determinant obtained from a separate orbital optimization has a large impact , as the DS reference is usually lower in energy than

Molecule	Experiment	NOCIS	STEX (dif. from NOCIS)	1C-NOCIS (dif. from NOCIS)
HO_2 O(1s)	528.6	529.022	1.259	0.000
N_2^+ N(1s)	-	394.800	3.414	-0.036
C_2H_3 C(1s)	-	283.002	0.951	0.089
NO N(1s)	399.7	400.593	0.807	0
NO O(1s)	532.7	532.857	0.000	0
NO_2 N(1s)	401.04	401.886	0.000	0
NO_2 O(1s)	530.32	530.135	0.001	0.001
OH O(1s)	525.8	526.883	1.548	0
CH3 C(1s)	281.35	282.637	0.808	0
CN C(1s)	-	280.537	0.841	0
CN N(1s)	-	393.404	0.741	0
HCO C(1s)	-	285.823	0.680	0
HCO O(1s)	-	531.213	0.427	0
N_2O^+ O(1s)	-	528.943	1.234	0
CO_2^+ C(1s)	-	290.997	0.000	0
CO_2^+ O(1s)	-	527.253	0.604	-0.137
MSE from NOCIS		-	0.832	-0.012
RMSE from NOCIS		-	1.163	0.035
RMSE from Expt.		0.809	1.595	0.809

TABLE IV. A comparison of NOCIS doublet K-edge energies and STEX K-edge and 1C-NOCIS differences in the aug-cc-pCVTZ basis set, and a further comparison to available experimental data. Mean signed error (MSE) and root mean square error (RMSE) are included. A 0 in the 1C-NOCIS column indicates that 1C-NOCIS and NOCIS are identical in that case.

a core-to-virtual excitation, and would be expected to play a large role in core excitations. This is further borne out in cases where the DS state does not play a large role in the K-edge due to symmetry, such as the NO O 1s K-edge. In this case, the K-edge is not a DS excitation, and NOCIS and STEX results are identical.

Molecule	NOCIS	STEX	1C-NOCIS
O_2 O(1s)	532.784	1.146	0.027
CH_2 C(1s)	285.274	0.864	0
NH N(1s)	399.233	1.225	0
CH_3N N(1s)	408.604	0.752	0
HCF C(1s)	286.762	2.027	0
HCF F(1s)	688.240	0.534	0
HCCl C(1s)	293.396	0.756	0
F_2C C(1s)	287.956	0.971	0
F_2C F(1s)	687.485	0.622	0.000
Cl_2C C(1s)	295.463	0.532	0
MSE		0.957	0.003
RMSE		0.997	0.008

TABLE V. A comparison of NOCIS triplet K-edge energies and STEX K-edge and 1C-NOCIS differences in the 6-31G basis set. Mean signed error (MSE) and root mean square error (RMSE) are included. A 0 in the 1C-NOCIS column indicates that 1C-NOCIS and NOCIS are identical in that case.

1C-NOCIS provides a significant improvement over STEX, with its error relative to NOCIS being an order of magnitude smaller. This data also exposes a second item of note: some of these numbers are lower than the NOCIS results. This can be explained by realizing that both STEX and 1C-NOCIS break spatial symmetry. STEX and 1C-NOCIS do not allow localized states to mix.

In sum, for doublet molecules, 1C-NOCIS provides a relatively substantial increase in accuracy for a reasonable computational cost, which can be especially valuable when potential molecules of interest have K-edges that are very close in energy. If accurate spatial symmetry is desired, the only option of these three methods is NOCIS.

As in the doublet case, for triplet molecules with with single core-hole references, 1C-NOCIS and NOCIS are identical. The comparison results in the 6-31G[64,65] and aug-cc-pCVTZ basis sets can be seen in Tables 5 and 6, respectively. Due to a lack of experimental

Molecule	NOCIS	STEX	1C-NOCIS
O_2 O(1s)	530.338	1.265	0.016
CH_2 C(1s)	282.526	0.736	0
NH N(1s)	396.266	1.079	0
CH_3N C(1s)	286.538	0.824	0
HCF C(1s)	283.996	0.888	0
HCF F(1s)	685.429	0.570	0
HCCl C(1s)	283.460	1.022	0
F_2C C(1s)	285.372	0.773	0
F_2C F(1s)	685.059	0.430	0.075
Cl_2C C(1s)	284.443	1.183	0
MSE		0.877	0.009
RMSE		0.912	0.024

TABLE VI. A comparison of NOCIS triplet K-edge energies and STEX K-edge and 1C-NOCIS differences in the aug-cc-pCVTZ basis set. Mean signed error (MSE) and root mean square error (RMSE) are included. A 0 in the 1C-NOCIS column indicates that 1C-NOCIS and NOCIS are identical in that case.

data, we have not included a comparison column. Our results are largely consistent with the results from doublets: with the addition of another DS excitation, the difference between NOCIS and STEX further increases. It appears that this difference is further exacerbated when the molecules are charged, which is why the doublet average errors are higher than the triplet ones.

When exploring the STEX + single core-hole reference implementation for doublet and triplet molecules, we found that it improved on STEX, but remained about 0.1 eV on average higher than 1C-NOCIS at a comparable cost. This is consistent with our expectation that the addition of the singly-occupied orbital reference would improve the results. This is effectively a Δ-SCF calculation using the DS-optimized determinant, and this method may not be suitable for higher excitations as there is no mixing between the DS state and the other core-to-valence determinants.

	Wall Time (s)			CPU Time (s)		
	1C-NOCIS	ADC	EOM-CCSD	1C-NOCIS	ADC	EOM-CCSD
Methyl	23.6	315.5	382.2	365.5	1420.4	939.5
Ethyl	103.6	1779.1	969.9	1615.9	16010.6	6399.3
1-propyl	345.1	14113	1988.8	5382.3	147203.7	17283.6
1-butyl	970.1	125374.6	5261.3	15235.1	1468947.2	60654.5

TABLE VII. A comparison of 1C-NOCIS, ADC-CVS(2)-x, and EOM-CCSD timings for computing core excited states of alkyl radicals. Calculations were done on Q-Chem 5.2[52], employing the cc-pCVDZ basis and run on 16 cores (on a 64 core node based on AMD Opteron 6134 processors running at a clock speed of 3.2 GHz).

B. Applications

1. *Computation Time*

While NOCIS calculations grow unfeasibly long starting around 4 reference atoms, 1C-NOCIS does not suffer from such constraints. Table VII presents timings for post-SCF 1C-NOCIS for doublet alkyl radicals in the cc-pCVDZ basis[66] (along with a comparison to ADC-CVS(2)-x and CVS-EOM-CCSD). We found a minimum 3-fold speedup in CPU time for one-center NOCIS versus ADC/EOM-CCSD, and a far greater comparative speedup when parallelization is introduced. We also note that 1C-NOCIS computed *all* core excited states while ADC/EOM-CCSD solved for only the first twenty. We note that the very high ADC timings resulted from the need to perform many hundreds (or even thousands) of iterations to converge roots. This suggests that 1C-NOCIS is an attractive method to use for larger molecules.

2. *TEMPO*

With the significantly decreased computational time of 1C-NOCIS, we are now able to generate K-edges for larger molecules. As an example, we look at (2,2,6,6-tetramethylpiperidin-1-yl)oxyl, more succinctly known as TEMPO. TEMPO and its fellow free radicals are widely

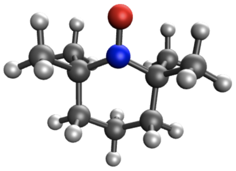

FIG. 3. (2,2,6,6-tetramethylpiperidin-1-yl)oxyl (TEMPO)

used in fields such as biochemistry and paramagnetic resonance spectroscopy, and may show promise for future use in medicine and organic synthesis[72]. With nine carbons, one nitrogen, and one oxygen, TEMPO is an ideal test for 1C-NOCIS.

For these calculations, we chose to use the recently developed SGM approach[46] to obtain the target core-ionized state energies. We used SGM instead of MOM for all our calculations of the C, N, and O K-edges of TEMPO, and the results can be seen in Figure 4. A comparison of the MOM and SGM results showed that both converged to identical ionized determinant energies. We used the cc-pCVDZ basis set.

Before discussing the results, it is first important to point out some features of the experimental spectra[72]. In the nitrogen spectrum, the second large peak at around 401.5 eV is actually the N_2 peak from the air, and so should not be seen in any calculated spectra. In the oxygen spectrum, the small peak next to the main peak at around 531 eV is the O_2 peak from the air, and should also not be seen in calculated spectra. All our spectra are simulated using a Voigt profile.

As can be seen from the comparisons, 1C-NOCIS agrees very well with the experimental spectra for TEMPO. It is somewhat puzzling, however, that the carbon spectrum requires a substantially larger shift than the nitrogen and oxygen ones. We have ruled out both relativistic and basis-set effects as the cause of this, and our hypothesis is that it is due to a difference in correlation. It is possible that the missing dynamic correlation is more significant for this system, and this is something we plan to explore further as we add dynamic correlation to our methods. Despite this, these results continue to provide encouragement for the use of 1C-NOCIS for use in identifying experimental spectra for doublet radicals.

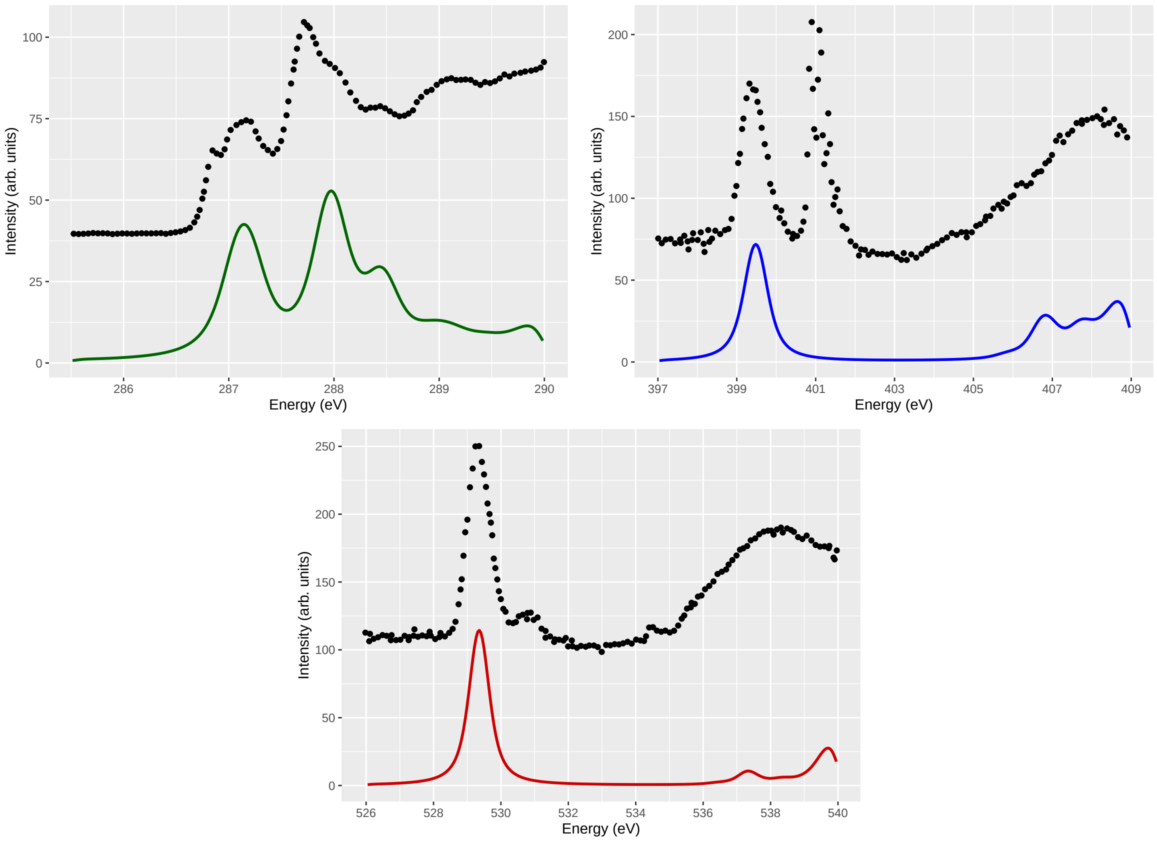

FIG. 4. A comparison of TEMPO experimental spectra (black)[72] to 1C-NOCIS spectra for the carbon (green), nitrogen (blue), and oxygen(red) K-edges. Calculated spectra are shifted (C -3.4 eV, N -1.2 eV, O -1.1 eV) and use Gaussian and Lorentzian broadening (.2 Gaussian, .25 Lorentzian for N and O, .1 Gaussian, .15 Lorentzian for C).

3. Singlet and Triplet States of MBA

As more NEXAFS spectra are taken, it will become increasingly useful to be able to distinguish between the ground singlet and excited triplet state of a molecule, for example in studying the signatures of electronic dynamics. To this end, we looked at the singlet versus triplet states of 4-mercaptobenzoic acid (MBA), which has been examined using XAS, but only in its solid state[73].

After optimizing the singlet and triplet state geometries separately, we then performed 1C-NOCIS calculations for the oxygen K-edge, again using the SGM algorithm. We used the cc-pCVDZ basis set. The results can be seen in Figure 6.

Triplet MBA has a distinctive lower energy peak that singlet MBA does not, which is a

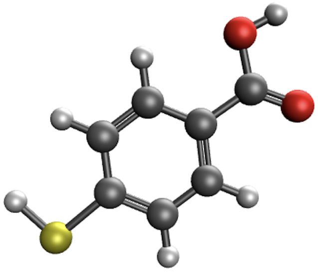

FIG. 5. 4-mercaptobenzoic acid (MBA), singlet geometry.

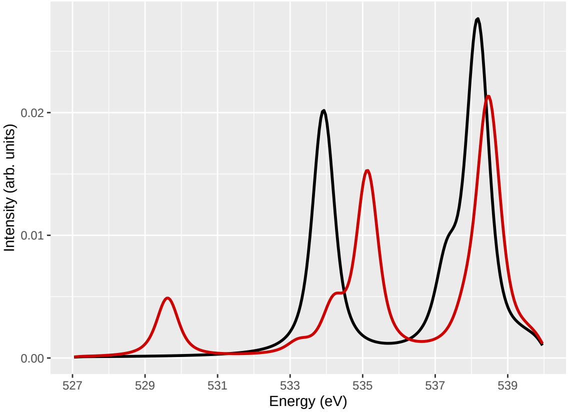

FIG. 6. A comparison of the 1C-NOCIS spectra for singlet (black) and triplet (red) MBA. Spectra use Gaussian and Lorentzian broadening (.2 G, .25 L).

signature that should be useful in identifying the presence of triplet MBA. The configuration of the excited state for the K-edge is the same for both the singlet and triplet species, so the peak shift is therefore a measure of the singlet-triplet splitting in the ground state.

Inspecting the available solid-state experimental spectrum[73] reveals that the general qualitative shape of the experimental curve is reproduced. However, the K edge of the triplet is either very faint or absent. It is possible that our intensity is overestimated or there are some experimental considerations that are unknown. It would be highly desirable to see gas-phase experiments for a direct assessment of the quality of our data.

IV. CONCLUSIONS

This paper explores the impact of varying levels of inclusion of non-orthogonality on core-excitation calculations, and also presents the implementation of one-center and triplet

NOCIS. Overall, we found that the impact of non-orthogonality increased as the number of singly-occupied orbitals increased, but that it had a limited effect on molecules with multiple of the same atom of interest. However, full NOCIS is the only method to retain spatial symmetry, so it is still recommended in cases where this is important.

This motivated the development of an approximation to NOCIS, 1C-NOCIS, which includes non-orthogonality only in regard to the core excitations to singly-occupied ground-state orbitals. 1C-NOCIS dramatically reduces the number of NOCI calculations, the method's computational bottleneck, and enables the treatment of far larger molecules than full NOCIS. Methods based on open-shell NOCIS provide a very promising framework for core-excited states. Extensions to include dynamical correlation and spin orbit coupling are promising future directions. Already, these methods provide a convenient way to simulate XAS spectra of first-row atoms in concert with experiment at an acceptable cost.

ACKNOWLEDGEMENTS

KJO thanks the members of the Head-Gordon group for fruitful discussions and Mickaël Delcey for the use of his spectrum plotting software. This work is supported by the Director, Office of Science, Office of Basic Energy Sciences of the US Department of Energy under contract No. DE-AC02-05CH11231.

[1] Martin-Diaconescu V, Kennepohl P. Sulfur K-edge XAS as a probe of sulfur-centered radical intermediates. J Am Chem Soc. 2007;129(11):3034–3035. Available from: `https://pubs.acs.org/doi/abs/10.1021/ja0676760`.

[2] Wang Z, Popolan-Vaida DM, Chen B, Moshammer K, Mohamed SY, Wang H, et al. Unraveling the structure and chemical mechanisms of highly oxygenated intermediates in oxidation of organic compounds. Proc Natl A Sci. 2017 Dec;114(50):13102–13107. Available from: `http://www.pnas.org/content/114/50/13102`.

[3] Nisoli M, Decleva P, Calegari F, Palacios A, Martín F. Attosecond Electron Dynamics in Molecules. American Chemical Society; 2017.

[4] Kraus PM, Zürch M, Cushing SK, Neumark DM, Leone SR. The ultrafast X-ray spectroscopic revolution in chemical dynamics. Nat Rev Chem. 2018 Jun;2(6):82–94.

[5] Milne CJ, Penfold TJ, Chergui M. Recent experimental and theoretical developments in time-resolved X-ray spectroscopies. Coord Chem Rev. 2014 Oct;277-278:44–68. Available from: `https://www.sciencedirect.com/science/article/pii/S0010854514000630`.

[6] Laffon C, Lasne J, Bournel F, Schulte K, Lacombe S, Parent P. Photochemistry of carbon monoxide and methanol in water and nitric acid hydrate ices: A NEXAFS study. Phys Chem Chem Phys. 2010 Sep;12(36):10865. Available from: `http://xlink.rsc.org/?DOI=c0cp00229a`.

[7] Norman P, Dreuw A. Simulating X-ray Spectroscopies and Calculating Core-Excited States of Molecules. Chem Rev. 2018 Aug;118(15):7208–7248. Available from: `https://pubs.acs.org/doi/10.1021/acs.chemrev.8b00156`.

[8] Sheehy JA, Gil TJ, Winstead CL, Farren RE, Langhoff PW. Correlation of molecular valence and K shell photoionization resonances with bond lengths . J Chem Phys. 1989 Aug;91(3):1796–1812.

[9] Triguero L, Pettersson L, Ågren H. Calculations of near-edge x-ray-absorption spectra of gas-phase and chemisorbed molecules by means of density-functional and transition-potential theory. Phys Rev B Condens Matter. 1998;58(12):8097–8110.

[10] Stener M, Fronzoni G, de Simone M. Time dependent density functional theory of core electrons excitations. Chem Phys Lett. 2003 May;373(1-2):115–123. Available from: `https://www.sciencedirect.com/science/article/pii/S0009261403005438`.

[11] Besley NA, Noble A. Time-dependent density functional theory study of the X-ray absorption spectroscopy of acetylene, ethylene, and benzene on Si(100). J Phys Chem C. 2007;111(8):3333–3340. Available from: `https://pubs.acs.org/doi/abs/10.1021/jp065160x`.

[12] DeBeer George S, Petrenko T, Neese F. Time-dependent density functional calculations of ligand K-edge X-ray absorption spectra. Inorg Chim Acta. 2008 Mar;361(4):965–972. Available from: `https://www.sciencedirect.com/science/article/pii/S0020169307003374?via{\%}3Dihub`.

[13] Ekström U, Norman P. X-ray absorption spectra from the resonant-convergent first-order polarization propagator approach. Phys Rev A. 2006 Oct;74(4):042722. Available from:

https://link.aps.org/doi/10.1103/PhysRevA.74.042722.

[14] Ekström U, Norman P, Carravetta V, Ågren H. Polarization Propagator for X-Ray Spectra. Phys Rev Lett. 2006 Oct;97(14):143001. Available from: https://link.aps.org/doi/10.1103/PhysRevLett.97.143001.

[15] Wang F, Ziegler T. Excitation energies of some d1 systems calculated using time-dependent density functional theory: an implementation of open-shell TDDFT theory for doublet-doublet excitations. Mol Phys. 2004 Dec;102(23-24):2585–2595. Available from: http://www.tandfonline.com/doi/abs/10.1080/0026897042000275080.

[16] Besley NA, Gilbert ATB, Gill PMW. Self-consistent-field calculations of core excited states. J Chem Phys. 2009 Mar;130(12):124308. Available from: http://aip.scitation.org/doi/10.1063/1.3092928.

[17] Krylov AI. Equation-of-Motion Coupled-Cluster Methods for Open-Shell and Electronically Excited Species: The Hitchhiker's Guide to Fock Space. Annu Rev Phys Chem. 2008 May;59(1):433–462. Available from: http://www.annualreviews.org/doi/10.1146/annurev.physchem.59.032607.093602.

[18] Monkhorst HJ. Calculation of properties with the coupled-cluster method. Int J Quantum Chem. 2009 Jun;12(S11):421–432. Available from: http://doi.wiley.com/10.1002/qua.560120850.

[19] Sadybekov A, Krylov AI. Coupled-cluster based approach for core-level states in condensed phase: Theory and application to different protonated forms of aqueous glycine. J Chem Phys. 2017 Jul;147(1):014107. Available from: http://aip.scitation.org/doi/10.1063/1.4990564.

[20] Coriani S, Christiansen O, Fransson T, Norman P. Coupled-cluster response theory for near-edge x-ray-absorption fine structure of atoms and molecules. Phys Rev A. 2012 Feb;85(2):022507. Available from: https://link.aps.org/doi/10.1103/PhysRevA.85.022507.

[21] Fransson T, Coriani S, Christiansen O, Norman P. Carbon X-ray absorption spectra of fluoroethenes and acetone: A study at the coupled cluster, density functional, and static-exchange levels of theory. J Chem Phys. 2013 Mar;138(12):124311. Available from: http://aip.scitation.org/doi/10.1063/1.4795835.

[22] List NH, Coriani S, Kongsted J, Christiansen O. Lanczos-driven coupledcluster damped linear response theory for molecules in polarizable environments. J Chem Phys. 2014 Dec;141(24):244107. Available from: `http://aip.scitation.org/doi/10.1063/1.4903981`.

[23] Peng B, Lestrange PJ, Goings JJ, Caricato M, Li X. Energy-Specific Equation-of-Motion Coupled-Cluster Methods for High-Energy Excited States: Application to K -edge X-ray Absorption Spectroscopy. J Chem Theory Comput. 2015 Sep;11(9):4146–4153. Available from: `http://pubs.acs.org/doi/10.1021/acs.jctc.5b00459`.

[24] Nooijen M, Bartlett RJ. Description of coreexcitation spectra by the openshell electronattachment equationofmotion coupled cluster method. J Chem Phys. 1995 May;102(17):6735–6756. Available from: `http://aip.scitation.org/doi/10.1063/1.469147`.

[25] Coriani S, Koch H. Communication: X-ray absorption spectra and core-ionization potentials within a core-valence separated coupled cluster framework. J Chem Phys. 2015 Nov;143(18):181103. Available from: `http://aip.scitation.org/doi/10.1063/1.4935712`.

[26] Zheng X, Cheng L. Performance of Delta-Coupled-Cluster Methods for Calculations of Core-Ionization Energies of First-Row Elements. J Chem Theory Comput. 2019 Sep;15(9):4945–4955. Available from: `https://pubs.acs.org/doi/10.1021/acs.jctc.9b00568`.

[27] Liu J, Matthews D, Coriani S, Cheng L. Benchmark Calculations of K-Edge Ionization Energies for First-Row Elements Using Scalar-Relativistic CoreValence-Separated Equation-of-Motion Coupled-Cluster Methods. J Chem Theory Comput. 2019 Mar;15(3):1642–1651. Available from: `https://pubs.acs.org/doi/10.1021/acs.jctc.8b01160`.

[28] Vidal ML, Feng X, Epifanovsky E, Krylov AI, Coriani S. New and Efficient Equation-of-Motion Coupled-Cluster Framework for Core-Excited and Core-Ionized States. J Chem Theory Comput. 2019 May;15(5):3117–3133. Available from: `https://pubs.acs.org/doi/10.1021/acs.jctc.9b00039`.

[29] Cederbaum LS, Domcke W, Schirmer J, von Niessen W. Many-Body Effects in Valence and Core Photoionization of Molecules. Phys Scr. 1980 Jan;21(3-4):481–491. Available from: `http://stacks.iop.org/1402-4896/21/i=3-4/a=040?key=crossref.fc0af20f0a199ef5aabf9d8f8d1731b5`.

[30] Barth A, Cederbaum LS. Many-body theory of core-valence excitations. Phys Rev A. 1981 Mar;23(3):1038–1061. Available from: `https://link.aps.org/doi/10.1103/PhysRevA.23.1038`.

[31] Barth A, Schirmer J. Theoretical core-level excitation spectra of N 2 and CO by a new polarisation propagator method. J Phys B: At Mol Phys. 1985 Mar;18(5):867–885. Available from: `http://stacks.iop.org/0022-3700/18/i=5/a=008?key=crossref.46749b8fe06ac01b9b8608e255f117a0`.

[32] Plekan O, Feyer V, Richter R, Coreno M, de Simone M, Prince KC, et al. A theoretical and experimental study of the near edge X-ray absorption fine structure (NEXAFS) and X-ray photoelectron spectra (XPS) of nucleobases: Thymine and adenine. Chem Phys. 2008 May;347(1-3):360–375. Available from: `https://www.sciencedirect.com/science/article/pii/S0301010407004302?via{\%}3Dihub`.

[33] Feyer V, Plekan O, Richter R, Coreno M, Vall-llosera G, Prince KC, et al. Tautomerism in Cytosine and Uracil: An Experimental and Theoretical Core Level Spectroscopic Study. J Phys Chem A. 2009 May;113(19):5736–5742. Available from: `http://pubs.acs.org/doi/abs/10.1021/jp900998a`.

[34] Wenzel J, Holzer A, Wormit M, Dreuw A. Analysis and comparison of CVS-ADC approaches up to third order for the calculation of core-excited states. J Chem Phys. 2015 Jun;142(21):214104. Available from: `http://aip.scitation.org/doi/10.1063/1.4921841`.

[35] Wenzel J, Wormit M, Dreuw A. Calculating X-ray Absorption Spectra of Open-Shell Molecules with the Unrestricted Algebraic-Diagrammatic Construction Scheme for the Polarization Propagator. J Chem Theory Comput. 2014 Oct;10(10):4583–4598. Available from: `http://pubs.acs.org/doi/10.1021/ct5006888`.

[36] Foresman JB, Head-Gordon M, Pople JA, Frisch MJ. Toward a systematic molecular orbital theory for excited states. J Phys Chem. 1992 Jan;96(1):135–149. Available from: `http://pubs.acs.org/doi/abs/10.1021/j100180a030`.

[37] Head-Gordon M, Grana AM, Maurice D, White CA. Analysis of Electronic Transitions as the Difference of Electron Attachment and Detachment Densities. J Phys Chem. 1995 Sep;99(39):14261–14270. Available from: `http://pubs.acs.org/doi/abs/10.1021/j100039a012`.

[38] Roemelt M, Maganas D, DeBeer S, Neese F. A combined DFT and restricted open-shell configuration interaction method including spin-orbit coupling: Application to transition metal L-edge X-ray absorption spectroscopy. J Chem Phys. 2013 May;138(20):204101. Available from: `http://aip.scitation.org/doi/10.1063/1.4804607`.

[39] Hunt WJ, Goddard WA. Excited States of H2O using improved virtual orbitals. Chem Phys Lett. 1969;3(6):414–418.

[40] Ågren H, Carravetta V, Vahtras O, Pettersson LGM. Direct, atomic orbital, static exchange calculations of photoabsorption spectra of large molecules and clusters. Chem Phys Lett. 1994 May;222(1-2):75–81.

[41] Ågren H, Carravetta V, Vahtras O, Pettersson LGM. Direct SCF direct static-exchange calculations of electronic spectra. Theor Chem Acc. 1997 Oct;97(1-4):14–40. Available from: `http://link.springer.com/10.1007/s002140050234`.

[42] Oosterbaan KJ, White AF, Head-Gordon M. Non-orthogonal configuration interaction with single substitutions for the calculation of core-excited states. J Chem Phys. 2018 Jul;149(4):044116. Available from: `http://aip.scitation.org/doi/10.1063/1.5023051`.

[43] Oosterbaan KJ, White AF, Head-Gordon M. Erratum: Non-orthogonal configuration interaction with single substitutions for the calculation of core-excited states (Journal of Chemical Physics (2018) 149 (044116) DOI: 10.1063/1.5023051). AIP Publishing LLC; 2018. Available from: `http://aip.scitation.org/doi/10.1063/1.5056181`.

[44] Oosterbaan KJ, White AF, Head-Gordon M. Non-Orthogonal Configuration Interaction with Single Substitutions for Core-Excited States: An Extension to Doublet Radicals. J Chem Theory Comput. 2019 May;15(5):2966–2973.

[45] Gilbert ATB, Besley NA, Gill PMW. Self-consistent field calculations of excited states using the maximum overlap method (MOM). J Phys Chem A. 2008 Dec;112(50):13164–13171. Available from: `http://pubs.acs.org/doi/abs/10.1021/jp801738f`.

[46] Hait D, Head-Gordon M. Excited state orbital optimization via minimizing the square of the gradient: General approach and application to singly and doubly excited states via density functional theory. J Chem Theory Comput. 2020 Feb;16(3):1699–1710.

[47] Thom AJW, Head-Gordon M. Hartree-Fock solutions as a quasidiabatic basis for nonorthogonal configuration interaction. J Chem Phys. 2009;131:124113. Available from: `https://doi.org/10.1063/1.3236841`.

[48] Maurice D, Head-Gordon M. On the nature of electronic transitions in radicals: an extended single excitation configuration interaction method. J Phys Chem. 1996 Jan;100(15):6131–6137. Available from: `http://pubs.acs.org/doi/abs/10.1021/jp952754j`.

[49] Ågren H, Yang L, Carravetta V, Pettersson LGM. On the interpretation of the NEXAFS spectrum of molecular oxygen. Chem Phys Lett. 1996 Aug;259(1-2):21–27.

[50] Yost SR, Head-Gordon M. Efficient Implementation of NOCI-MP2 Using the Resolution of the Identity Approximation with Application to Charged Dimers and Long C-C Bonds in Ethane Derivatives. J Chem Theory Comput. 2018 Sep;14(9):4791–4805. Available from: `http://pubs.acs.org/doi/10.1021/acs.jctc.8b00697`.

[51] Evangelista F, Carravetta V, Stefani G, Jansik B, Alagia M, Stranges S, et al. Electronic structure of copper phthalocyanine: An experimental and theoretical study of occupied and unoccupied levels. J Chem Phys. 2007 Mar;126(12):124709. Available from: `http://aip.scitation.org/doi/10.1063/1.2712435`.

[52] Shao Y, Gan Z, Epifanovsky E, Gilbert ATB, Wormit M, Kussmann J, et al. Advances in molecular quantum chemistry contained in the Q-Chem 4 program package. Mol Phys. 2015 Jan;113(2):184–215. Available from: `http://www.tandfonline.com/doi/abs/10.1080/00268976.2014.952696`.

[53] Sanderson C, Curtin R. Armadillo: a template-based C++ library for linear algebra. J Open Source Softw. 2016;1(2):26.

[54] Sundstrom EJ, Head-Gordon M. Non-orthogonal configuration interaction for the calculation of multielectron excited states. J Chem Phys. 2014 Mar;140(11):114103. Available from: `http://aip.scitation.org/doi/10.1063/1.4868120`.

[55] NIST. CCCBDB calculated geometries; 2018. Available from: `https://cccbdb.nist.gov/geom1x.asp`.

[56] Becke AD. Densityfunctional thermochemistry. III. The role of exact exchange. J Chem Phys. 1993 Apr;98(7):5648–5652. Available from: `http://aip.scitation.org/doi/10.1063/1.464913`.

[57] Lee C, Yang W, Parr RG. Development of the Colle-Salvetti correlation-energy formula into a functional of the electron density. Phys Rev B. 1988 Jan;37(2):785–789. Available from: `https://link.aps.org/doi/10.1103/PhysRevB.37.785`.

[58] Vosko SH, Wilk L, Nusair M. Accurate spin-dependent electron liquid correlation energies for local spin density calculations: a critical analysis. Can J Phys. 1980 Aug;58(8):1200–1211. Available from: `http://www.nrcresearchpress.com/doi/10.1139/p80-159`.

[59] Weigend F, Ahlrichs R. Balanced basis sets of split valence, triple zeta valence and quadruple zeta valence quality for H to Rn: Design and assessment of accuracy. Phys Chem Chem Phys. 2005 Aug;7(18):3297. Available from: `http://xlink.rsc.org/?DOI=b508541a`.

[60] Hitchcock AP, Brion CE. K-shell excitation spectra of CO, N2 and O2. J Electron Spectrosc Relat Phenom. 1980 Jan;18(1):1–21.

[61] Hitchcock AP, Brion CE. K-shell excitation of HF and F2 studied by electron energy-loss spectroscopy. J Phys B: At Mol Phys. 1981;14(22):4399.

[62] Hitchcock AP, Brion CE. Carbon K-shell excitation of C2H2, C2H4, C2H6 and C6H6 by 2.5 keV electron impact. J Electron Spectrosc Relat Phenom. 1977 Jan;10(3):317–330.

[63] Barrus DM, Blake RL, Burek AJ, Chambers KC, Pregenzer AL. K-shell photoabsorption coefficients of O2, CO2, CO, and N2O. Phys Rev A. 1979 Sep;20(3):1045–1061.

[64] Ditchfield R, Hehre WJ, Pople JA. Self-Consistent Molecular-Orbital Methods. IX. An Extended Gaussian-Type Basis for MolecularOrbital Studies of Organic Molecules. J Chem Phys. 1971 Jan;54(2):724–728.

[65] Hehre WJ, Ditchfield K, Pople JA. Self-consistent molecular orbital methods. XII. Further extensions of gaussian-type basis sets for use in molecular orbital studies of organic molecules. J Chem Phys. 1972;56(5):2257–2261.

[66] Dunning TH. Gaussian basis sets for use in correlated molecular calculations. I. The atoms boron through neon and hydrogen. J Chem Phys. 1989 Jan;90(2):1007–1023. Available from: `http://aip.scitation.org/doi/10.1063/1.456153`.

[67] Kendall RA, Dunning TH, Harrison RJ. Electron affinities of the first-row atoms revisited. Systematic basis sets and wave functions. J Chem Phys. 1992 May;96(9):6796–6806. Available from: `http://aip.scitation.org/doi/10.1063/1.462569`.

[68] Woon DE, Dunning TH. Gaussian basis sets for use in correlated molecular calculations. V. Core-valence basis sets for boron through neon. J Chem Phys. 1995 Sep;103(11):4572–4585. Available from: `http://aip.scitation.org/doi/10.1063/1.470645`.

[69] Wight GR, Brion CE. K-shell excitations in NO and O2 by 2.5 keV electron impact. J Electron Spectrosc Relat Phenom. 1974 Jan;4(4):313–325.

[70] Zhang W, Sze KH, Brion CE, Tong XM, Li JM. Inner-shell electron energy loss spectra of NO2 at high resolution: Comparison with multichannel quantum defect calculations of dipole oscillator strengths and transition energies. Chem Phys. 1990 Jan;140(2):265–279.

[71] Alagia M, Lavollée M, Richter R, Ekström U, Carravetta V, Stranges D, et al. Probing the potential energy surface by high-resolution x-ray absorption spectroscopy: The umbrella motion of the core-excited C H3 free radical. Physical Review A - Atomic, Molecular, and Optical Physics. 2007 Aug;76(2):022509.

[72] Ljubić I, Kivimäki A, Coreno M. An experimental NEXAFS and computational TDDFT and ΔdFT study of the gas-phase core excitation spectra of nitroxide free radical TEMPO and its analogues. Phys Chem Chem Phys. 2016 Apr;18(15):10207–10217.

[73] Hraya A, Inui H, Yamahira S, Takahash O. X-ray absorption spectra of excited triplet states of organic molecules. In: J. Phys. Conf. Ser.. vol. 875. Institute of Physics Publishing; 2017. .

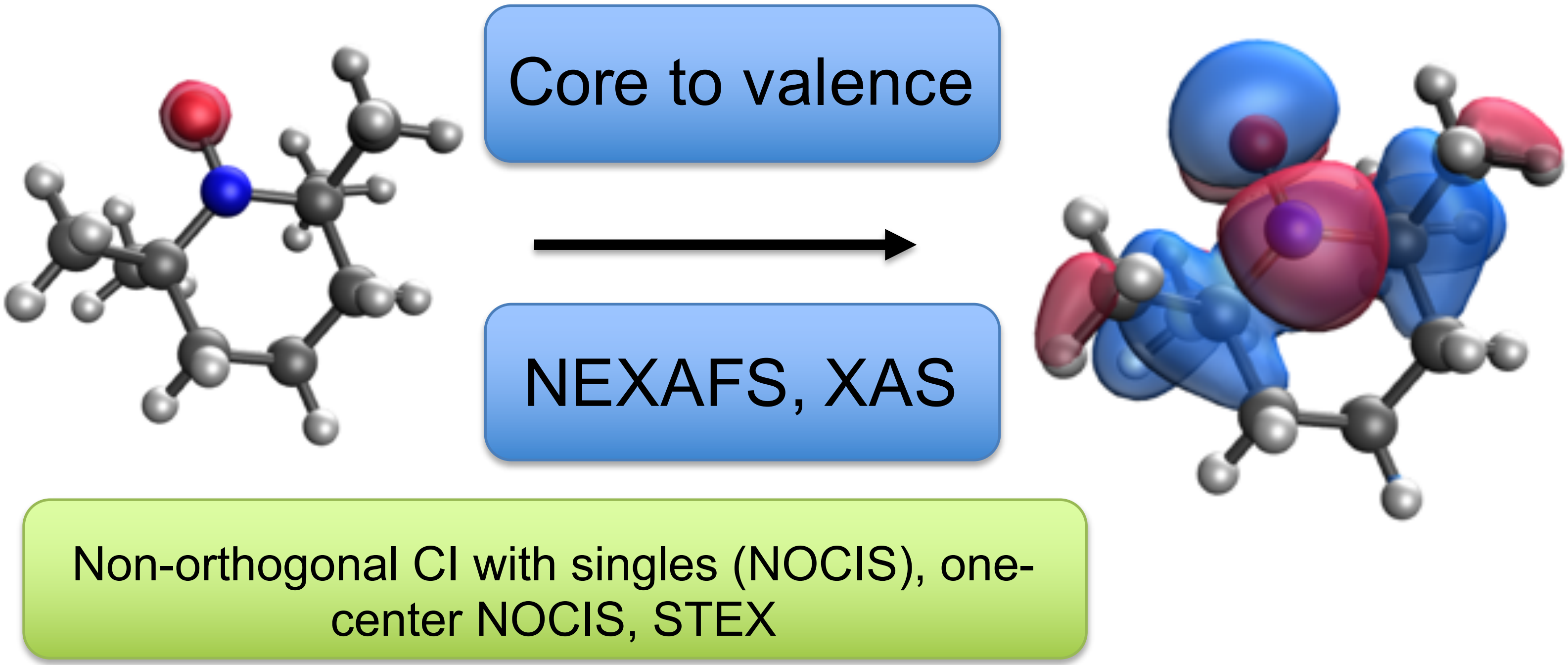

Core to valence

NEXAFS, XAS

Non-orthogonal CI with singles (NOCIS), one-center NOCIS, STEX